

Ruthenium(II) Polypyridyl Complexes: Potential Precursors, Metalloligands, and Topo II Inhibitors

Sanjeev Sharma, Sanjay K. Singh, and Daya S. Pandey*

Department of Chemistry, Faculty of Science, Banaras Hindu University, Varanasi 221 005, U.P., India

Received July 31, 2007

Neutral and cationic mononuclear complexes containing both group 15 and polypyridyl ligands [Ru(κ^3 -tptz)(PPh₃-Cl₂)] [1; tptz = 2,4,6-tris(2-pyridyl)-1,3,5-triazine], [Ru(κ^3 -tptz)(κ^2 -dppm)Cl]BF₄ [2; dppm = bis(diphenylphosphino)methane], [Ru(κ^3 -tptz)(PPh₃)(pa)Cl] (3; pa = phenylalanine), [Ru(κ^3 -tptz)(PPh₃)(dtc)Cl] (4; dtc = diethyldithiocarbamate), [Ru(κ^3 -tptz)(PPh₃)(SCN)₂] (5) and [Ru(κ^3 -tptz)(PPh₃)(N₃)₂] (6) have been synthesized. Complex 1 has been used as a metalloligand in the synthesis of homo- and heterodinuclear complexes [Cl₂(PPh₃)Ru(μ -tptz)Ru(η^6 -C₆H₆)Cl]BF₄ (7), [Cl₂(PPh₃)Ru(μ -tptz)Ru(η^6 -C₁₀H₁₄)Cl]PF₆ (8), and [Cl₂(PPh₃)Ru(μ -tptz)Rh(η^5 -C₅Me₅)Cl]BF₄ (9). Complexes 7–9 present examples of homo- and heterodinuclear complexes in which a typical organometallic moiety [(η^6 -C₆H₆)RuCl]⁺, [(η^6 -C₁₀H₁₄)RuCl]⁺, or [(η^5 -C₅Me₅)RhCl]⁺ is bonded to a ruthenium(II) polypyridine moiety. The complexes have been fully characterized by elemental analyses, fast-atom-bombardment mass spectroscopy, NMR (¹H and ³¹P), and electronic spectral studies. Molecular structures of 1–3, 8, and 9 have been determined by single-crystal X-ray diffraction analyses. Complex 1 functions as a good precursor in the synthesis of other ruthenium(II) complexes and as a metalloligand. All of the complexes under study exhibit inhibitory effects on the Topoisomerase II–DNA activity of filarial parasite *Setaria cervi* and β -hematin/hemozoin formation in the presence of *Plasmodium yoelii* lysate.

Introduction

There has been an increasing interest in ruthenium(II) polypyridine chemistry. The principal reason behind this surge in research on ruthenium(II) polypyridyl complexes is their peculiar electrochemical and photophysical properties.¹ These complexes find wide applications in several research fields such as conversion of solar energy,² fabrication of molecular devices,³ DNA intercalation,⁴ and protein binding.⁵ In addition, mono- and dinuclear ruthenium(II) polypyridyl complexes have been widely used as electrochemiluminescence luminophores.⁶ It has been observed that the ligand present in such systems plays a crucial role

in determining and eventually improving both the light-emitting and electron-transfer performances.⁷ In this direction, a large number of neutral⁸ and anionic⁹ ligands have been included in the coordination sphere of ruthenium(II) polypyridyl metal fragments. Among the polypyridyl ligands, 2,4,6-tris(2-pyridyl)-1,3,5-triazine (tptz) has drawn special attention. In general, tptz functions as a tridentate ligand,

* To whom correspondence should be addressed. E-mail: dspbhu@bhu.ac.in.

(1) (a) Lehn, J.-M. *Supramolecular Chemistry*; VCH: Weinheim, Germany, 1995. (b) Balzani, V.; Ceroni, P.; Juris, A.; Venturi, M.; Campagna, S.; Puntariero, F.; Serroni, S. *Coord. Chem. Rev.* **2001**, *219*, 545. (c) Beyeler, A.; Belsler, P. *Coord. Chem. Rev.* **2002**, *230*, 28. (d) Campagna, S.; Pietro, P. D.; Loiseau, F.; Maubert, B.; McClenaghan, N.; Passalacqua, R.; Puntariero, F.; Ricevuto, V.; Serroni, S. *Coord. Chem. Rev.* **2002**, *229*, 67. (e) Balzani, V.; Campagna, S.; Denti, G.; Juris, A.; Serroni, S.; Venturi, M. *Acc. Chem. Res.* **1998**, *31*, 26. (f) Slate, C. A.; Striplin, D. R.; Moss, J. A.; Chen, P.; Erickson, B. W.; Meyer, T. J. *J. Am. Chem. Soc.* **1998**, *120*, 4885.

(2) (a) Amouyal, E. *Sol. Energy Mater. Sol. Cells* **1995**, *38*, 249. (b) Puntariero, F.; Serroni, S.; Galletta, M.; Juris, A.; Licciardello, A.; Chiorboli, C.; Campagna, S.; Scandola, F. *ChemPhysChem* **2005**, *6*, 129. (c) Kelly, C. A.; Meyer, G. J. *Coord. Chem. Rev.* **2001**, *211*, 295. (d) Dürr, H.; Bossmann, S. *Acc. Chem. Res.* **2001**, *34*, 905. (e) Bignozzi, C. A.; Argazzi, R.; Kleverlaan, C. J. *Chem. Soc. Rev.* **2000**, *29*, 87. (f) Blanco, M.-J.; Jiménez, M. C.; Chambron, J.-C.; Heitz, V.; Linke, M.; Sauvage, J.-P. *Chem. Soc. Rev.* **1999**, *28*, 293. (g) Kalyanasundaram, K.; Grätzel, M. *Coord. Chem. Rev.* **1998**, *177*, 347. (h) Cola, L. D.; Belsler, P. *Coord. Chem. Rev.* **1998**, *177*, 301.

(3) (a) Damrauer, N. H.; Cerullo, G.; Yeh, A.; Boussie, T. R.; Shank, C. V.; McCusker, J. K. *Science* **1997**, *275*, 54. (b) Carter, F. L.; Siatkowski, R. E.; Wohltjn, H. *Molecular Electronics Devices*; North Holland: Amsterdam, The Netherlands, 1988. (c) Balzani, V.; Credi, A.; Venturi, M. *Molecular Devices and Machines—A Journey into the Nano World*; Wiley-VCH: Weinheim, Germany, 2003. (d) Robertson, N.; McGowan, C. A. *Chem. Soc. Rev.* **2003**, *32*, 96. (e) Balzani, V.; Credi, A.; Raymo, F. M.; Stoddart, J. F. *Angew. Chem., Int. Ed.* **2000**, *39*, 3348.

forming mononuclear complexes.¹⁰ However, in some cases it simultaneously functions as tridentate and bidentate ligands.¹¹ Also, there is one report dealing with the trinucleating mode of tptz.¹²

Although extensive studies have been made on ruthenium complexes containing polypyridyl ligands, complexes containing both group 15 and polypyridyl ligands, wherein group 15 ligands stabilize ruthenium(II) forms, have not been extensively studied.¹³ Recently, a series of cationic ruthenium(II) complexes with the formulations $[\text{Ru}(\kappa^3\text{-L})(\text{EPh}_3)_2\text{-Cl}]^+$ [L = tptz or 2,2':6,6'-terpyridine (tpy); E = P and As] and analogous osmium(II) complexes $[\text{Os}(\kappa^3\text{-tptz})(\text{EPh}_3)_2\text{-Cl}]^+$ (E = P and As) containing both group 15 and polypyridyl ligands were synthesized.¹⁴ Various studies established that the complexes $[\text{Ru}(\kappa^3\text{-L})(\text{EPh}_3)_2\text{Cl}]^+$ have the potential to behave as good precursors in the synthesis of other ruthenium complexes under mild reaction conditions can act as potential *metalloligands* in the synthesis of homo(hetero)di(poly)nuclear complexes and also act as biocatalysts.^{14a}

In an extension of our earlier studies devoted in this direction, we have synthesized neutral complex $[\text{Ru}(\kappa^3\text{-tptz})(\text{PPh}_3)_2\text{Cl}_2]$ from the reactions of $[\text{RuCl}_2(\text{PPh}_3)_3]$ with tptz in benzene under refluxing conditions. The neutral complex $[\text{Ru}(\kappa^3\text{-tptz})(\text{PPh}_3)_2\text{Cl}_2]$ also possesses a κ^3 -bonded tptz, tertiary phosphine, and labile chloro groups analogous to the complexes of the series $[\text{Ru}(\kappa^3\text{-L})(\text{EPh}_3)_2\text{Cl}]^+$. Because of the presence of the polar chloro groups bound to the ruthenium center and uncoordinated donor groups on almost planar tptz, the complexes of this series are expected to exhibit a rich variety of chemistry, have the potential to behave as *metalloligands*, and can act as biocatalysts. We devoted our efforts in this direction, have isolated complexes containing both the group 15 and polypyridyl ligands, and have examined its use as a precursor, *metalloligand*, and biocatalyst.

In this work, we have adopted a multispect approach toward the complex $[\text{Ru}(\kappa^3\text{-tptz})(\text{PPh}_3)_2\text{Cl}_2]$ (**1**) and present herein its reproducible synthesis, its potential use as a precursor, and its applicability in the synthesis of homo- and heterodinuclear complexes. Further, we report herein the inhibitory effect of the complexes on the DNA–Topoisomerase II (Topo II) activity of filarial parasite *Setaria cervi* and on the β -hematin/hemozoin formation in the presence of *Plasmodium yoelii* lysate.

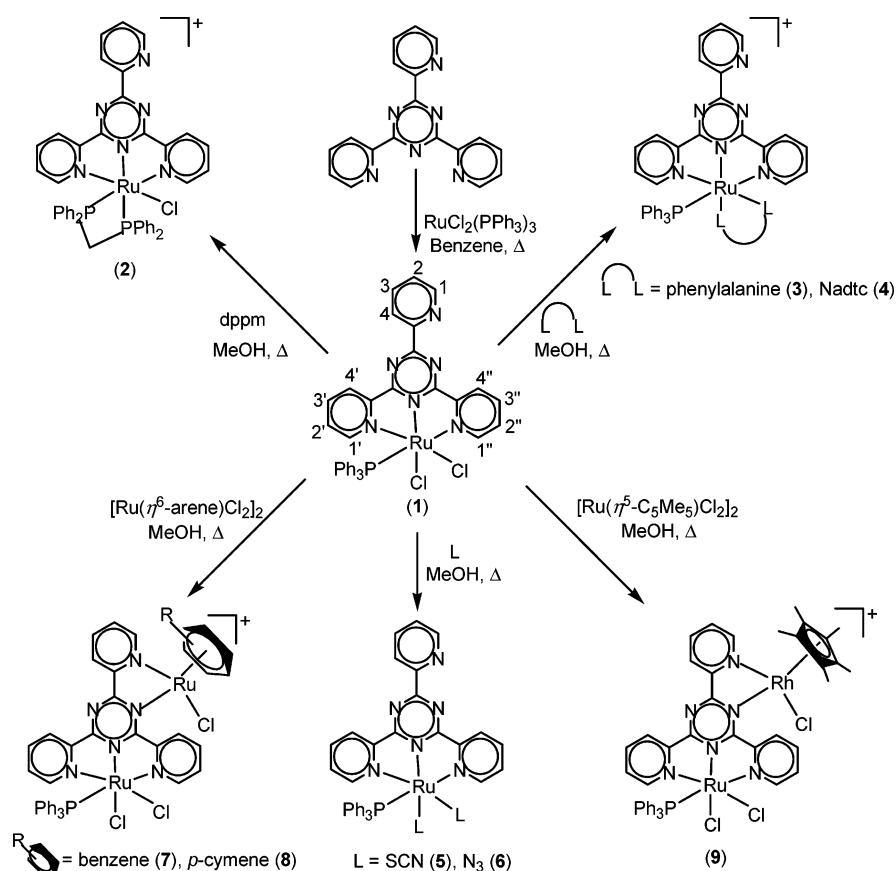
Results and Discussion

Scheme 1 shows the synthetic route for the synthesis of air-stable neutral complex **1** and its derivatives. Complex **1** was used as a precursor in the synthesis of mononuclear complexes $[\text{Ru}(\kappa^3\text{-tptz})(\kappa^2\text{-dppm})\text{Cl}]\text{BF}_4$ [**2**; dppm = bis-(diphenylphosphino)methane], $[\text{Ru}(\kappa^3\text{-tptz})(\text{PPh}_3)(\text{pa})]\text{Cl}$ (**3**; pa = phenylalanine), $[\text{Ru}(\kappa^3\text{-tptz})(\text{PPh}_3)(\text{dte})]\text{Cl}$ (**4**; dte = diethyldithiocarbamate), $[\text{Ru}(\kappa^3\text{-tptz})(\text{PPh}_3)(\text{SCN})_2]$ (**5**), and $[\text{Ru}(\kappa^3\text{-tptz})(\text{PPh}_3)(\text{N}_3)_2]$ (**6**). Complexes **2–6** were obtained in excellent yield from the reaction of **1** with respective bases in methanol under refluxing conditions. The formation of

- (4) (a) Gupta, N.; Grover, N.; Neyhart, G. A.; Singh, P.; Thorp, H. H. *Inorg. Chem.* **1993**, *32*, 310. (b) Erkkila, K. E.; Odom, D. T.; Barton, J. K. *Chem. Rev.* **1999**, *29*, 2777. (c) Kelly, J. M.; Tossi, A. B.; McConnell, D. J.; OhUigin, C. *Nucl. Acids Res.* **1985**, *13*, 6017. (d) Ambrose, A.; Maiya, B. G. *Inorg. Chem.* **2000**, *39*, 4264. (e) Miao, R.; Mongelli, M. T.; Zigler, D. F.; Winkel, B. S. J.; Brewer, K. J. *Inorg. Chem.* **2006**, *45*, 10413. (f) van der Schilden, K.; Garcia, F.; Kooijman, H.; Spek, A. L.; Haasnoot, J. G.; Reedijk, J. *Angew. Chem., Int. Ed.* **2004**, *43*, 5668. (g) Beck, J. L.; Zhang, P.-X.; Ji, L.-N. *Dalton Trans.* **2003**, 2260. (h) Xu, H.; Zheng, K.-C.; Chen, Y.; Li, Y.-Z.; Lin, L.-J.; Li, H.; Zhang, P.-X.; Ji, L.-N. *Dalton Trans.* **2003**, 2260. (i) Puckett, C. A.; Barton, J. K. *J. Am. Chem. Soc.* **2007**, *129*, 46. (j) Liu, X. W.; Li, J.; Deng, H.; Zheng, K. C.; Mao, Z. W.; Ji, L. N. *Inorg. Chim. Acta* **2005**, *358*, 3311.
- (5) (a) Yang, X.-J.; Drepper, F.; Wu, B.; Sun, W.-H.; Haehnel, W.; Janiak, C. *Dalton Trans.* **2005**, 256. (b) Karidi, K.; Garoufis, A.; Hadjiliadis, N.; Reedijk, J. *Dalton Trans.* **2005**, 728. (c) Hofmeier, H.; Pahnke, J.; Weidl, C. H.; Schubert, U. S. *Biomacromolecules* **2004**, *5*, 2055 and references cited therein.
- (6) (a) Richter, M. M. *Chem. Rev.* **2004**, *104*, 3003. (b) Miao, W. J.; Bard, A. J. *Anal. Chem.* **2004**, *76*, 7109. (c) Welter, S.; Brunner, K.; Hofstra, J. W.; De Cola, L. *Nature* **2003**, *421*, 54. (d) Liu, C.-Y.; Bard, A. J. *J. Am. Chem. Soc.* **2002**, *124*, 4190. (e) Liu, C.-Y.; Bard, A. J. *Acc. Chem. Res.* **1999**, *32*, 235.
- (7) (a) Elsevier, C. J.; Reedijk, J.; Walton, P. H.; Ward, M. D. *Dalton Trans.* **2003**, 1869. (b) Demadis, K. D.; Hartshorn, C. M.; Meyer, T. J. *Chem. Rev.* **2001**, *101*, 2655. (c) Kaim, W.; Klein, A.; Glöckle, M. *Acc. Chem. Res.* **2000**, *33*, 755.
- (8) (a) Balzani, V.; Juris, A.; Venturi, M.; Campagna, S.; Serroni, S. *Chem. Rev.* **1996**, *96*, 759. (b) Newkome, G. R.; Patri, A. K.; Holder, E.; Schubert, U. S. *Eur. J. Org. Chem.* **2004**, 235. (c) Medlycott, E. A.; Hanan, G. S. *Chem. Soc. Rev.* **2005**, *34*, 133. (d) Hofmeier, H.; Schubert, U. S. *Chem. Soc. Rev.* **2004**, *33*, 373. (e) Zong, R.; Thummel, R. P. *J. Am. Chem. Soc.* **2004**, *126*, 10800. (f) Bergman, S. D.; Goldberg, I.; Barbieri, A.; Barigelletti, F.; Kol, M. *Inorg. Chem.* **2004**, *43*, 2355.
- (9) (a) Frayssé, S.; Coudret, C.; Launay, J. P. *J. Am. Chem. Soc.* **2003**, *125*, 5880. (b) Launay, J. P. *Chem. Soc. Rev.* **2001**, *30*, 386. (c) Sondaz, E.; Jaud, J.; Launay, J.-P.; Bonvoisin, J. *Eur. J. Inorg. Chem.* **2002**, 1924. (d) Sondaz, E.; Gourdon, A.; Launay, J. P.; Bonvoisin, J. *Inorg. Chim. Acta* **2001**, *316*, 79. (e) Crutchley, R. J. *Coord. Chem. Rev.* **2001**, *219*, 125.
- (10) (a) Embry, W. A.; Ayres, G. H. *Anal. Chem.* **1968**, *40*, 1499. (b) Janmohamed, M. J.; Ayres, G. H. *Anal. Chem.* **1972**, *44*, 2263. (c) Warren, R. N.; Watton, E. C. *Aust. J. Chem.* **1969**, *22*, 1499. (d) Pagenkopf, G. K.; Margerum, D. W. *Inorg. Chem.* **1968**, *7*, 2514. (e) Collins, P.; Diehl, H.; Smith, G. F. *Anal. Chem.* **1959**, *31*, 1862. (f) Arif, A. M.; Hart, F. A.; Hursthouse, M. B.; Thornton-Pett, M.; Zhu, W. J. *Chem. Soc., Dalton Trans.* **1984**, 2449. (g) Sedney, D.; Kahjehassiri, M.; Reiff, W. M. *Inorg. Chem.* **1981**, *20*, 3476. (h) Berger, R. M.; Holcombe, J. R. *Inorg. Chim. Acta* **1995**, *232*, 217. (i) Polson, M. I. J.; Medlycott, E. A.; Hanan, G. S.; Mikelsons, L.; Taylor, N. J.; Watanabe, M.; Tanaka, Y.; Loiseau, F.; Passalacqua, R.; Campagna, S. *Chem.—Eur. J.* **2004**, *10*, 3640. (j) Metcalfe, C. M.; Spey, S.; Adams, H.; Thomas, J. A. *J. Chem. Soc., Dalton Trans.* **2002**, 4732. (k) Saji, T.; Aoyagui, S. *J. Electroanal. Chem.* **1980**, *110*, 329. (l) Tokel-Takvoryan, N. E.; Hemingway, R. E.; Bard, A. J. *J. Am. Chem. Soc.* **1973**, *95*, 6582. (m) Paul, P.; Tyagi, B.; Bhadbhade, M. M.; Suresh, E. J. *Chem. Soc., Dalton Trans.* **1997**, 2273. (n) Lin, C. T.; Bottcher, W.; Chou, M.; Creutz, C.; Sutin, N. *J. Am. Chem. Soc.* **1976**, *98*, 6536. (o) Lalrempuia, R.; Govindaswamy, P.; Mozharivskiy, Y. A.; Kollipara, M. R. *Polyhedron* **2004**, *23*, 1069.
- (11) (a) Halfpenny, J.; Small, R. W. H. *Acta Crystallogr.* **1982**, *B38*, 939. (b) Thomas, N. C.; Foley, B. L.; Rheingold, A. L. *Inorg. Chem.* **1988**, *27*, 3426. (c) Berger, R. M.; Ellis, D. D. *Inorg. Chim. Acta* **1996**, *241*, 1. (d) Ghumaan, S.; Kar, S.; Mobin, S. M.; Harish, B.; Puranik, V. G.; Lahiri, G. K. *Inorg. Chem.* **2006**, *45*, 2413.

- (12) Yenmez, I.; Specker, H. *Fresenius' Z. Anal. Chem.* **1979**, 296, 140.
- (13) (a) Sullivan, B. P.; Calvert, J. M.; Meyer, T. J. *Inorg. Chem.* **1980**, *19*, 1404. (b) Perez, W. J.; Lake, C. H.; See, R. F.; Toomey, L. M.; Churchill, M. R.; Takeuchi, K. J.; Radano, C. P.; Boyko, W. J.; Bessel, C. A. *J. Chem. Soc., Dalton Trans.* **1999**, 2281.
- (14) (a) Sharma, S.; Chandra, M.; Pandey, D. S. *Eur. J. Inorg. Chem.* **2004**, *17*, 3555. (b) Chandra, M.; Sahay, A. N.; Pandey, D. S.; Tripathi, R. P.; Saxena, J. K.; Reddy, V. J. M.; Puerta, M. C.; Valerga, P. J. *Organomet. Chem.* **2004**, *689*, 2256. (c) Sharma, S.; Singh, S. K.; Chandra, M.; Pandey, D. S. *J. Inorg. Biochem.* **2005**, *99*, 458. (d) Singh, S. K.; Sharma, S.; Chandra, M.; Pandey, D. S. *J. Organomet. Chem.* **2005**, *690*, 3105.

Scheme 1



1–3 has been authenticated by single-crystal X-ray diffraction analyses (vide supra). Complex **4** has also been synthesized by the reaction of $[\text{Ru}(\kappa^3\text{-tptz})(\text{PPh}_3)_2\text{Cl}]\text{BF}_4$ with sodium diethyldithiocarbamate in refluxing methanol and has been structurally characterized.^{14a}

Complex **1** behaves as a *metalloligand* and reacted with the chloro-bridged dimeric arene (arene = benzene and *p*-cymene) ruthenium complexes $[\{\eta^6\text{-C}_6\text{H}_6\}\text{Ru}(\mu\text{-Cl})\text{Cl}_2]$ and $[\{\eta^6\text{-C}_{10}\text{H}_{14}\}\text{Ru}(\mu\text{-Cl})\text{Cl}_2]$ and isostructural rhodium complex $[\{\eta^5\text{-C}_5\text{Me}_5\}\text{Rh}(\mu\text{-Cl})\text{Cl}_2]$ in a 2:1 molar ratio to afford homo- and heterodinuclear complexes $[\text{Cl}_2(\text{PPh}_3)\text{Ru}(\mu\text{-tptz})\text{Ru}(\eta^6\text{-C}_6\text{H}_6)\text{Cl}]\text{BF}_4$ (**7**), $[\text{Cl}_2(\text{PPh}_3)\text{Ru}(\mu\text{-tptz})\text{Ru}(\eta^6\text{-C}_{10}\text{H}_{14})\text{Cl}]\text{PF}_6$ (**8**), and $[\text{Cl}_2(\text{PPh}_3)\text{Ru}(\mu\text{-tptz})\text{Rh}(\eta^5\text{-C}_5\text{Me}_5)\text{Cl}]\text{BF}_4$ (**9**) in pretty good yield. The formation of **8** and **9** has been authenticated crystallographically. Complexes **7–9** present unique examples wherein typical organometallic fragments, viz., $[\eta^6\text{-C}_6\text{H}_6]\text{RuCl}^+$, $[\eta^6\text{-C}_{10}\text{H}_{14}]\text{RuCl}^+$, or $[\eta^5\text{-C}_5\text{Me}_5]\text{RhCl}^+$, are coordinated to the ruthenium(II) polypyridine fragment $[\text{Ru}(\kappa^3\text{-tptz})]$. All of the complexes were characterized by satisfactory elemental analyses. Information about the composition of the complexes was also obtained from fast-atom-bombardment mass spectroscopy (FAB-MS). FAB-MS spectra of the representative mono- and dinuclear complexes **4**, **5**, **8**, and **9** are shown in parts a–d of Figure 1, and data with the assignments are recorded in the Experimental Section. The overall fragmentation patterns and the presence of various peaks in the FAB-MS spectra strongly supported the formulation of the respective mono- and dinuclear complexes.

X-ray Crystallography. Molecular structures of **1–3**, **8**, and **9** have been determined crystallographically. The complexes crystallize in $P2_1/c$ (**1**), $P2_1/n$ (**2**), $P\bar{1}$ (**3**), $P12_1/n_1$ (**8**), and $P2_1$ (**9**) space groups. Details about data collection, refinement, and structure solution are recorded in Table 1, and selected geometrical parameters are collected in Table 2. Crystal structures of **1–3**, **8**, and **9** with atom-numbering schemes are shown in Figure 2a–e. The coordination geometry about the ruthenium in the mononuclear complexes **1–3** is distorted octahedral. In complex **1**, ruthenium is bonded with the major coordination sites of tptz through pyridyl nitrogen atoms N1 and N3 and triazolyl nitrogen N2 from the central triazine ring in a κ^3 manner, P1 from triphenylphosphine, and the chloro groups Cl1 and Cl2, while in complex **2**, both of the phosphorus atoms P1 and P2 from dppm and the chloro group Cl1 are bonded to the ruthenium center along with tptz through its pyridyl nitrogen atoms (N1 and N3) and central triazolyl nitrogen N2 in a κ^3 manner. In complex **3**, arrangement of tptz is analogous to that in **1** and **2** and other positions are occupied by phosphorus P1 from PPh_3 , amino nitrogen N7, and carboxyl oxygen O1 of the coordinated pa.

The angles N1–Ru1–N2 and N2–Ru1–N3 in **1** are essentially equal to 79.02(7) and 78.83(7)°, while in **2** and **3**, these are 77.14(15), 76.95(15)° and 78.48(12), 79.02(12)°, respectively. This suggests inward bending of the coordinated pyridyl group and may be the reason for the observed distortion.^{14a} Distortion from the regular octahedral geometry is further reflected by intraligand trans angles N1–Ru1–

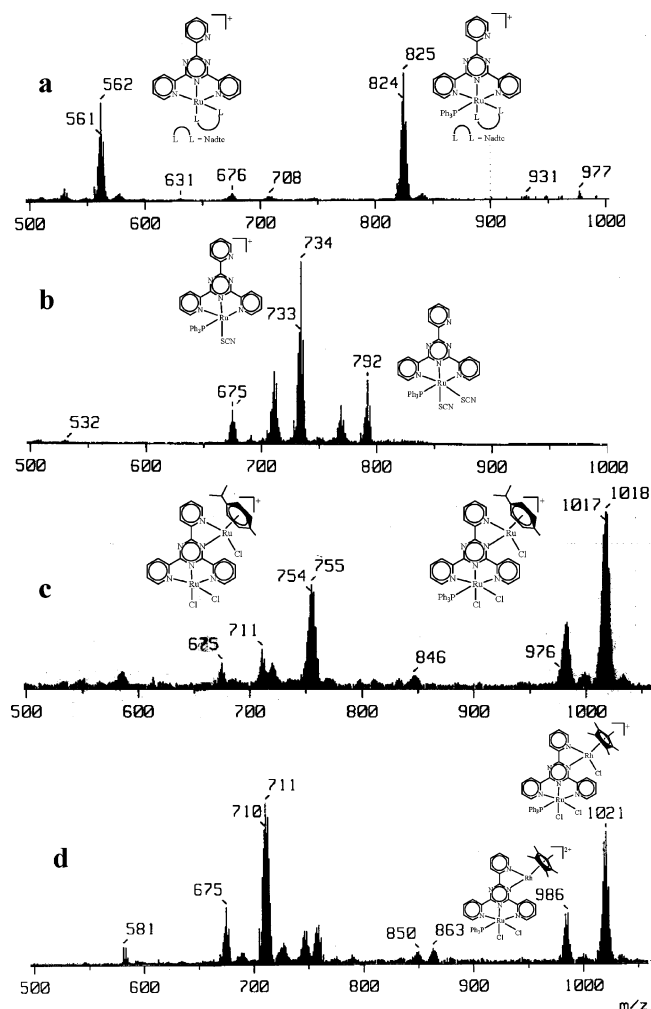


Figure 1. FAB-MS spectra with peak assignments for **4** (a), **5** (b), **8** (c), and **9** (d).

N3 in **1–3**, which are 157.00(7), 154.08(16), and 157.16(12) $^\circ$, respectively. The other two interligand trans angles C11–Ru1–P1 and C12–Ru1–N2 are 176.82(2) and 174.22(5) $^\circ$ in **1**, the angles C11–Ru1–P1 and N2–Ru1–P2 are 167.92(5) and 178.05(11) $^\circ$ in **2**, and the angles N8–Ru1–P1 and N2–Ru1–O1 are 172.58(9) and 171.66(5) $^\circ$ in **3**, respectively. The angle C12–Ru1–C11 in **1** is 90.02(3) $^\circ$, which suggested that the chloro groups are cis-disposed. The Ru–P and Ru–Cl distances are normal and consistent with the values reported in other related complexes.^{14a,15} The Ru1 to central triazine nitrogen bond length Ru1–N2 in **1** is 1.9234(17) Å, which is smaller than the Ru1 to coordinated pyridyl nitrogen bond lengths Ru1–N1 [2.0921(17) Å] and Ru1–N3 [2.0846(17) Å]. Similarly, the Ru1–N2 bond distance in **2** is 2.018(4) Å and the Ru1–N1 and Ru1–N3 distances are 2.112(4) and 2.124(4) Å, respectively, while the Ru1–N2 bond distance in **3** is 1.921(3) Å and the Ru1–N1 and Ru1–N3 distances are 2.078(3) and 2.103(3) Å. The Ru–N bond distances are consistent with κ^3 coordination of tptz and comparable to those in other Ru^{II}tptz

complexes.^{14a,b,16} Uncoordinated pyridyl rings in **1–3** are inclined at 18.1, 31.6, and 18.6 $^\circ$, respectively, from the central triazine ring plane.

An interesting structural feature of the homodinuclear complex **8** and heterodinuclear complex **9** is the coordination of $[(\eta^6\text{-C}_{10}\text{H}_{14})\text{RuCl}]^+$ and $[(\eta^6\text{-C}_5\text{Me}_5)\text{RhCl}]^+$ moieties, respectively, through the uncoordinated nitrogen atoms N4 and N6 of the tptz bonded to ruthenium in complex **1**. The coordination geometry about Ru1 in both complexes **8** and **9** is the same as that in **1**; the only difference lies about Ru2 and Rh1. Ru2 in **8** is bonded through triazine nitrogen N4, pyridyl nitrogen N6, one chloro group, and the *p*-cymene ring (C37–C42) in a η^6 manner. Similarly, Rh1 in **9** is coordinated through triazine nitrogen N4, pyridyl nitrogen N6 of the tptz in a κ^2 manner, one chloro group, and the pentamethylcyclopentadienyl (Cp*) ring (C37–C41) in a η^5 manner. Typical “piano-stool” geometry about Ru2 in **8** and Rh1 in **9** is maintained. The *p*-cymene ring in **8** is planar, the average Ru–C distance is 2.02(8) Å [range 2.176(9)–2.216(10) Å], and the Ru2 to *p*-cymene ring centroid bond distance is 1.685 Å, which is comparable to the distances reported in other ruthenium *p*-cymene complexes.¹⁷ The Cp* ring in **9** is planar with an average Rh–C distance of 2.6512 Å, and the Rh center is displaced by 1.785 Å from the centroid of the Cp* ring. The C–C bond lengths within the Cp* ring and C–Me distances are normal.¹⁸ Rh–N and Rh–Cl bond lengths are consistent with the values reported in the literature.^{18a,19}

Crystal structures of **1–3**, **8**, and **9** revealed the presence of extensive intra- and intermolecular C–H \cdots X (X = N, Cl, and F) and C–H \cdots π interactions. Matrixes of the intermolecular interactions for **1–3**, **8**, and **9** are shown in Table S1 in the Supporting Information. It is well-established that these types of interactions play an important role in the construction of huge supramolecular architectures.²⁰ Weak interaction studies in **1** show face-to-face C–H \cdots π interactions, leading to a single helical motif, which is interlinked to another helical motif through C–H \cdots N interaction, giving

- (16) Paul, P.; Tyagi, B.; Bilakhia, A. K.; Dastidar, P.; Suresh, E. *Inorg. Chem.* **2000**, *39*, 14.
- (17) Singh, S. K.; Trivedi, M.; Chandra, M.; Sahay, A. N.; Pandey, D. S. *Inorg. Chem.* **2004**, *43*, 8600 and references cited therein.
- (18) (a) Chandra, M.; Sahay, A. N.; Mobin, S. M.; Pandey, D. S. *J. Organomet. Chem.* **2005**, *690*, 3105. (b) Singh, S. K.; Chandra, M.; Dubey, S. K.; Pandey, D. S. *Eur. J. Inorg. Chem.* **2006**, 3954. (c) Hughes, R. P.; Lindner, D. C.; Liable-Sands, L. M.; Rheingold, A. L. *Organometallics* **2001**, *20*, 363. (d) Scheiring, T.; Fiedler, J.; Kaim, W. *Organometallics* **2001**, *20*, 1437.
- (19) (a) Paul, P.; Tyagi, B.; Bilakhia, A. K.; Parthasarthy, D.; Bhadbhade, M. M.; Suresh, E.; Ramchandriah, G. *Inorg. Chem.* **1998**, *37*, 5733. (b) Aneetha, H.; Zacharias, P. S.; Srinivas, B.; Lee, G. H.; Wang, Y. *Polyhedron* **1998**, *18*, 299.
- (20) (a) Braga, D.; Grepioni, F.; Tedesco, E. *Organometallics* **1998**, *17*, 2669. (b) Desiraju, G. R.; Steiner, T. *Weak Hydrogen Bonds in Structural Chemistry and Biology*; Oxford University Press: Oxford, U.K., 1999. (c) Steiner, T. *Angew. Chem., Int. Ed.* **2002**, *41*, 48. (d) Hobza, P.; Havlas, Z. *Chem. Rev.* **2000**, *100*, 4253. (e) Zhang, J.-P.; Lin, Y.-Y.; Huang, X.-C.; Chen, X.-M. *Inorg. Chem.* **2005**, *44*, 3146. (f) Desiraju, G. R. *J. Chem. Soc., Dalton Trans.* **2000**, 3745. (g) Lü, X.-Q.; Jiang, J.-J.; Chen, C.-L.; Kang, B.-S.; Su, C.-Y. *Inorg. Chem.* **2005**, *44*, 4515. (h) Yin, H.; Lee, G. I.; Park, H. S.; Payne, G. A.; Rodriguez, J. M.; Sebtü, S. M.; Hamilton, A. D. *Angew. Chem., Int. Ed.* **2005**, *44*, 2704. (i) Hirschberg, J. H. K. K.; Brunsveld, L.; Ramzi, A.; Vekemans, J. A. J. M.; Sijbesma, R. P.; Meijer, E. W. *Nature* **2000**, *407*, 167.

(15) (a) Hayashida, T.; Nagashima, H. *Organometallics* **2002**, *21*, 3884. (b) Nishiyama, H.; Konno, M.; Aoki, K.; Davies, H. M. L.; Huw, M. L. *Organometallics* **2002**, *21*, 2536.

Table 1. Crystallographic Data for **1**, **2**, and **7–9**

	1	2	3	8	9
chemical formula	C ₃₆ H ₂₇ Cl ₂ N ₆ PRu	C ₄₃ H ₃₄ BClF ₄ N ₆ P ₂ Ru	C ₄₆ H ₃₉ Cl ₃ N ₇ O _{6.50} PRu	C ₄₆ H ₄₃ Cl ₃ F ₆ N ₆ OP ₂ Ru ₂	C ₄₆ H ₄₂ BCl ₃ F ₄ N ₆ OPRhRu
fw	746.58	920.03	1024.27	1180.29	1122.97
color, habit	blue, block	violet-black, block	violet-black, block	blue, block	blue, block
cryst size (mm)	0.35 × 0.27 × 0.21	0.33 × 0.28 × 0.26	0.33 × 0.26 × 0.21	0.35 × 0.26 × 0.23	0.34 × 0.28 × 0.21
space group	<i>P</i> 2 ₁ / <i>c</i>	<i>P</i> 2 ₁ / <i>n</i>	<i>P</i> 1	<i>P</i> 2 ₁ / <i>n</i>	<i>P</i> 2 ₁
cryst syst	monoclinic	monoclinic	triclinic	monoclinic	monoclinic
<i>a</i> (Å)	11.667(3)	12.024(2)	13.812(2)	17.031(3)	11.4272(4)
<i>b</i> (Å)	14.6718(6)	27.0339(12)	14.094(2)	18.042(4)	15.0419(14)
<i>c</i> (Å)	19.6465(17)	13.592(2)	14.2642(18)	17.038(3)	13.7625(12)
α (deg)	90	90	61.663(14)	90	90
β (deg)	105.461(14)	104.529(15)	82.940(11)	92.20(3)	98.124(5)
γ (deg)	90	90	71.920(13)	90	90
<i>V</i> (Å ³)	3241.3(10)	4277.1(11)	2322.3(6)	5231.5(18)	2341.9(3)
<i>Z</i>	4	4	2	4	2
<i>D</i> _{calc} (g cm ⁻³)	1.530	1.429	1.476	1.499	1.593
μ (mm ⁻¹)	0.735	0.560	0.602	0.852	0.939
<i>T</i> (K)	293(2)	293(2)	293(2)	293(2)	293(2)
no. of reflns	5683	7509	8156	9293	7727
no. of param	415	523	588	598	592
<i>R</i> factor all	0.0321	0.0954	0.0591	0.1016	0.0491
<i>R</i> factor [<i>I</i> > 2σ(<i>I</i>)]	0.0240	0.0500	0.0452	0.0776	0.0384
wR2	0.0607	0.1328	0.1288	0.1976	0.1064
wR2 [<i>I</i> > 2σ(<i>I</i>)]	0.0582	0.1183	0.1222	0.1770	0.0975
GOF	1.029	0.914	1.068	1.052	1.029

Table 2. Important Bond Parameters for **1**, **2**, **3**, **8** and **9**

	1	2	3	8	9				
Ru1–N1	2.0921(17)	Ru1–N1	2.112(4)	Ru1–N1	2.103(3)	Ru1–N1	2.065(6)	Ru1–N1	2.095(5)
Ru1–N2	1.9234(17)	Ru1–N2	2.018(4)	Ru1–N2	1.921(3)	Ru1–N2	1.918(5)	Ru1–N2	1.925(5)
Ru1–N3	2.0846(17)	Ru1–N3	2.124(4)	Ru1–N3	2.078(3)	Ru1–N3	2.056(6)	Ru1–N3	2.071(5)
Ru1–P1	2.3087(7)	Ru1–P1	2.2821(14)	Ru1–O1	2.119(3)	Ru1–P1	2.335(2)	Ru1–P1	2.3140(14)
Ru1–Cl1	2.4457(7)	Ru1–P2	2.3054(14)	Ru1–N7	2.137(3)	Ru1–Cl1	2.430(2)	Ru1–Cl1	2.4354(14)
Ru1–Cl2	2.4449(6)	Ru1–Cl1	2.4517(14)	Ru1–P1	2.3186(10)	Ru1–Cl2	2.4185(18)	Ru1–Cl2	2.4116(16)
						Ru2–N4	2.118(5)	Rh1–N4	2.190(4)
						Ru2–N6	2.083(6)	Rh1–N6	2.091(5)
						Ru2–C _{av}	2.200(9)	Rh1–C _{av}	2.1562(2)
						Ru2–C _{ct}	1.685	Rh1–C _{ct}	1.785
						Ru2–Cl3	2.394(2)	Rh1–Cl3	2.4004(17)
N1–Ru1–N2	79.02(7)	N1–Ru1–N2	77.14(15)	N1–Ru1–N2	78.48(12)	N1–Ru1–N2	78.8(2)	N1–Ru1–N2	79.4(2)
N1–Ru1–N3	157.00(7)	N1–Ru1–N3	154.08(16)	N1–Ru1–N3	157.16(12)	N1–Ru1–N3	158.4(2)	N1–Ru1–N3	157.68(18)
N2–Ru1–N3	78.83(7)	N2–Ru1–N3	76.95(15)	N2–Ru1–N3	79.02(12)	N2–Ru1–N3	79.6(2)	N2–Ru1–N3	78.51(19)
N2–Ru1–Cl2	174.22(5)	P1–Ru1–P2	71.83(5)	N2–Ru1–O1	171.66(11)	N2–Ru1–Cl2	173.83(17)	N2–Ru1–Cl2	173.57(16)
Cl1–Ru1–Cl2	90.02(3)	N2–Ru1–P2	178.05(11)	O1–Ru1–N7	78.52(11)	Cl1–Ru1–Cl2	88.17(8)	Cl1–Ru1–Cl2	89.28(6)
P1–Ru1–Cl1	176.82(2)	P1–Ru1–Cl1	167.92(5)	P1–Ru1–N7	172.58(9)	P1–Ru1–Cl1	178.84(8)	P1–Ru1–Cl1	176.37(6)
						N4–Ru2–N6	76.8(2)	N4–Rh1–N6	76.78(18)

a straight chain (Figure S1 in the Supporting Information), while in **2**, C–H···F and C–H···π interactions lead to an upstairslike motif (Figure 3).^{20b} In **9**, two types of edge-to-face C–H···π interactions have been found, leading to a single helical motif (Figure S2 in the Supporting Information).

NMR Studies. ¹H NMR spectral data of the complexes are recorded in the Experimental Section. The position and integrated intensity of various signals corresponding to tptz corroborated well to a system involving coordination of tptz with the ruthenium in a κ³ manner with two magnetically equivalent coordinated pyridyl rings and one uncoordinated pyridyl ring for mononuclear complexes.²¹ The ¹H NMR spectrum of **1** displays signals at δ 9.46 (d, 2H, *J* = 4.2 Hz, H_{1,1'}), 8.58 (d, 2H, *J* = 8.7 Hz, H_{4,4'}), 7.86 (t, 2H, *J* = 6.9 Hz, H_{2,2'}), and 7.58 (m, 3H, H_{3,3'}) corresponding to the protons of coordinated pyridyl rings and δ 8.95 (d, 1H, *J* = 2.7 Hz, H₁), 8.64 (d, 1H, H₄) 7.96 (t, 1H, *J* = 6.9 Hz, H₂),

and 7.53 (H₃) for pendant pyridyl protons of tptz (see Scheme 1 for numbering of the pyridyl protons). The aromatic protons of PPh₃ resonated as a broad multiplet in the region δ 7.36–7.10. The ¹H NMR spectra of **2–6** followed the general trends observed for **1**. The main feature of the ¹H NMR spectra of the dtc-containing complex **4** is the presence of multiplets in the upshielded side characteristic of methyl and methylene protons (see the Experimental Section).

However, in the dinuclear complexes **7–9**, coordination of a second metal center splits the equivalency of tptz pyridyl protons. ¹H NMR spectra of **8** show four deshielded peaks at δ 10.64, 9.41, 8.63, and 8.26 assignable to H₁, H₄, H₂, and H₃, respectively, corresponding to the pyridyl ring protons of tptz coordinated to [(η⁶-C₁₀H₁₄)RuCl]⁺. Also, chemical shifts for the pyridyl protons, which are in close proximity to [(η⁶-C₁₀H₁₄)RuCl]⁺, exhibited a downfield shift to a greater extent than the other protons (see the Experimental Section). A similar trend has been observed for **7** and **9** also. Characteristic signals for coordinated benzene (**7**), *p*-cymene (**8**), and pentamethylcyclopentadienyl (**9**)

(21) Chirayil, S.; Hegde, V.; Jahng, Y.; Thummel, R. P. *Inorg. Chem.* **1991**, *30*, 2821.

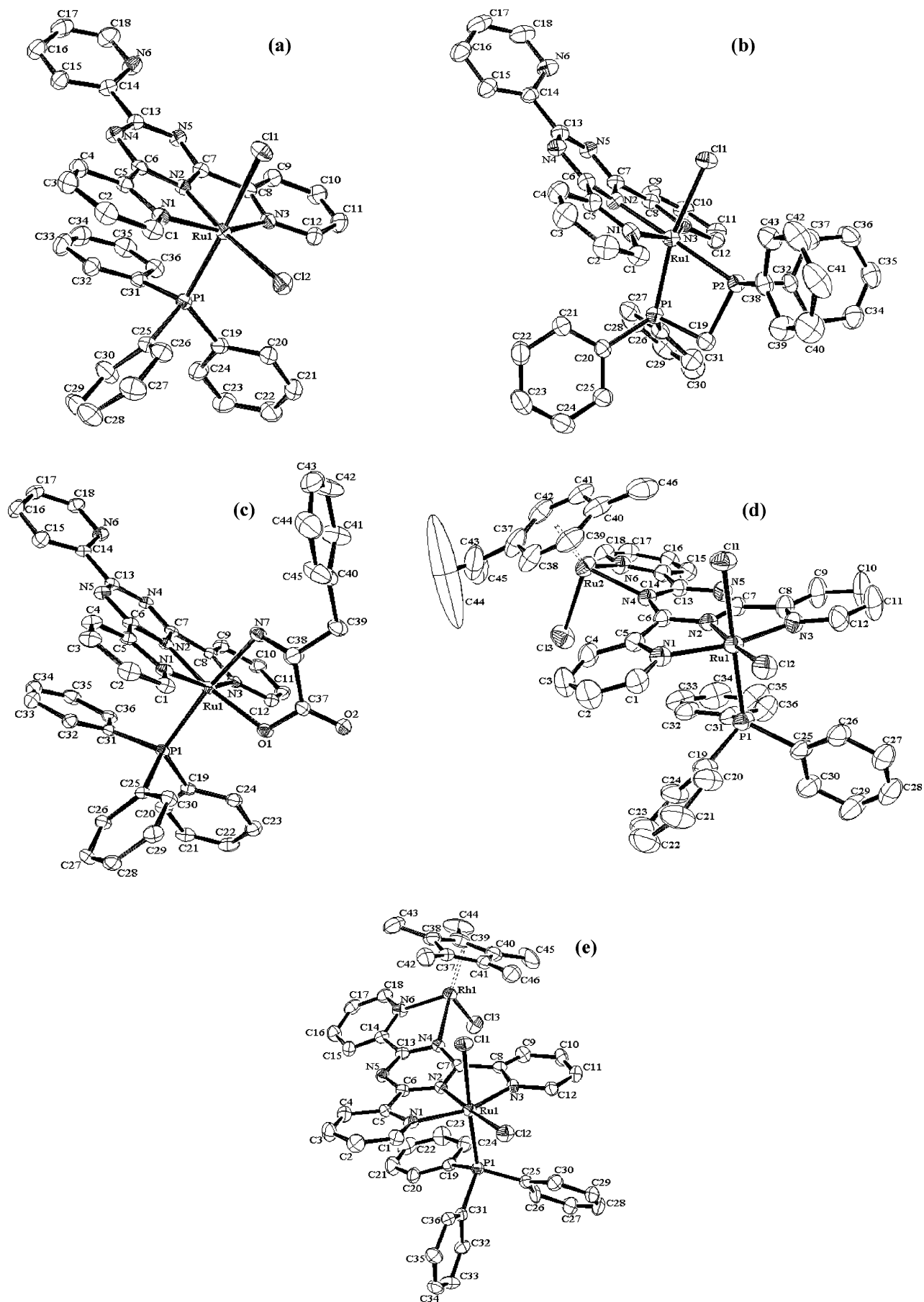


Figure 2. Molecular structures of complexes **1** (a), **2** (b), **3** (c), **8** (d), and **9** (e).

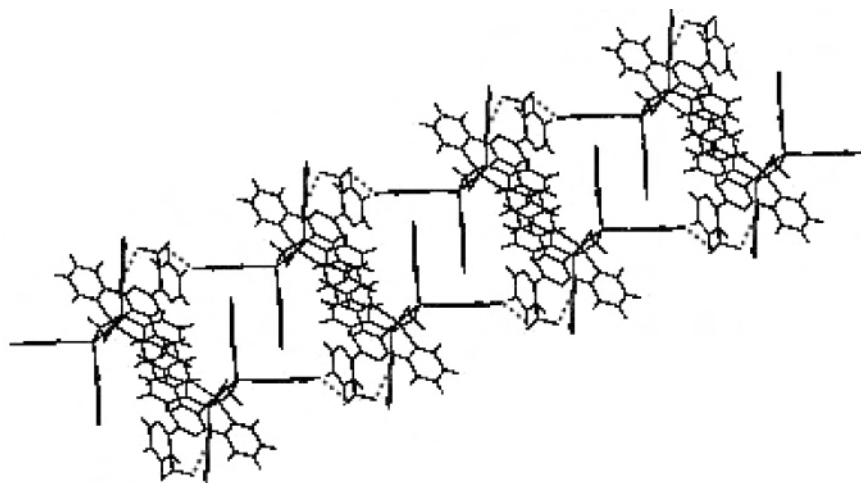


Figure 3. Face-to-face π - π and C-H...F interaction leading to an upstairs motif in complex **2**.

protons appeared at δ 5.82 (s, 6H, C₆H₆), 5.69 (m, 3H), 5.45 (d, 1H), 2.65 (m, 1H, CH(CH₃)₂), 2.12 (s, 3H, C-CH₃), 1.09 (d, 3H, CH(CH₃)₂), 0.92 (d, 3H, CH(CH₃)₂), and 1.45 (s, 15H, C₅(CH₃)₅).^{17,18b} The integrated intensity and position of the signals are consistent with the formulation of respective complexes.

Signals associated with the ³¹P NMR nuclei of the coordinated PPh₃ resonated as sharp singlets in the ³¹P NMR spectra of complexes **1** and **3–9** in the range of δ 27.89–40.77. Complex **2** displayed two doublets at δ 6.64 (d, J = 56.62 Hz) and -11.29 (d, J = 58.56 Hz) associated with the ³¹P NMR nuclei of the coordinated dppm.

UV–Vis Spectroscopy. UV–vis spectra of the complexes were acquired in dichloromethane, and spectral data are summarized in the Experimental Section. Electronic spectra of the mononuclear complexes **1–6** and dinuclear complexes **7–9** are depicted in Figure 4a,b. Ruthenium polypyridyl complexes usually show intense peaks in the UV region corresponding to ligand-based $\pi \rightarrow \pi^*$ transitions with overlapping metal-to-ligand charge-transfer (MLCT) transitions in the visible region.^{13a} An analogous general trend is observable in the electronic spectra of the complexes under study. Mononuclear complexes **1–6** displayed intense transitions in the UV–vis region. The lowest-energy absorption bands in the electronic spectra of **1–6** in the visible region at \sim 478–557 and 374–353 nm (except for complex **2**) on the basis of its intensity and position have been tentatively assigned to $d\pi_{\text{Ru}} \rightarrow \pi^*_{\text{tptz}}$ MLCT transitions. The bands in the high-energy side at \sim 280 nm have been assigned to ligand-centered $\pi \rightarrow \pi^*/n \rightarrow \pi^*$ transitions.²² The homo/heterodinuclear complexes **7–9** exhibited similar trends, with an additional band at \sim 405 nm that can be assigned to the MLCT band due to $d\pi_{\text{M-arene}} \rightarrow \pi^*_{\text{tptz}}$ transitions.^{18b} The higher-energy MLCT transitions of the dinuclear complexes exhibited significant red shifts compared to the parent complex **1**, which may be attributed to stabilization of the lowest unoccupied molecular orbital (LUMO) π^* level of tptz by its coordination to another metal center, leading to

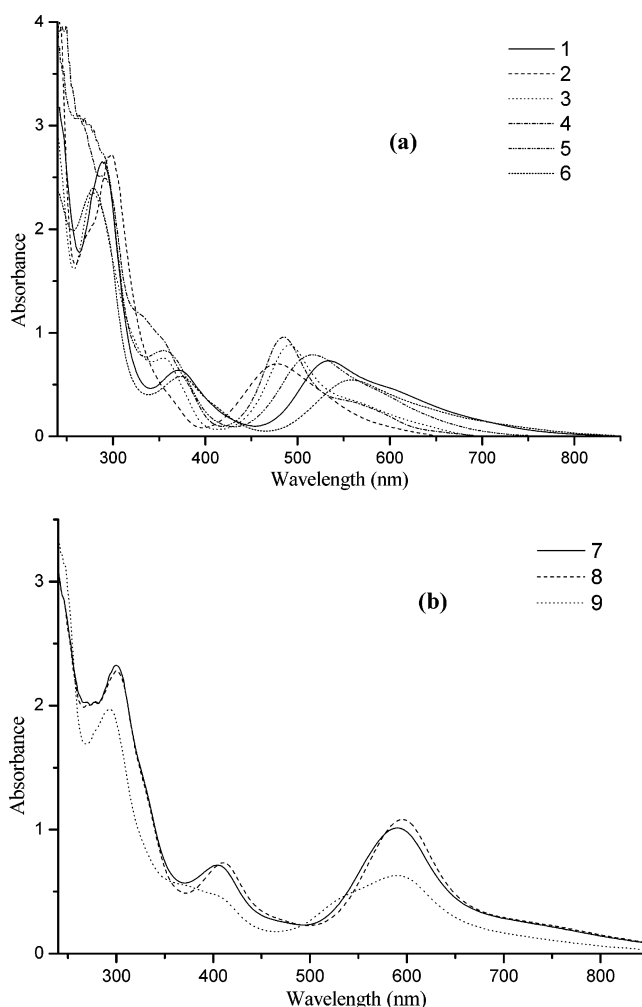


Figure 4. UV–vis spectra of mononuclear complexes **1–6** (a) and binuclear complexes **7–9** (b) in dichloromethane.

enhanced $d\pi \rightarrow \pi^*$ orbital overlap with a low highest occupied molecular orbital (HOMO)–LUMO energy gap.²³ It is further observed that substitution of the chloro groups in complex **1** by neutral or ionic bidentate ligands significantly destabilizes the π^* orbital of tptz, resulting in blue-shifted $d\pi_{\text{Ru}} \rightarrow \pi^*_{\text{tptz}}$ absorption bands. However, substitution

(22) (a) Didier, P.; Ortmans, I.; Mesmaeker, A. K.-D.; Watts, R. J. *Inorg. Chem.* **1993**, *32*, 5239. (b) Sullivan, B. P.; Salmon, D. J.; Meyer, T. *J. Inorg. Chem.* **1978**, *17*, 3334.

(23) Rillema, D. P.; Mack, K. B. *Inorg. Chem.* **1982**, *21*, 3849.

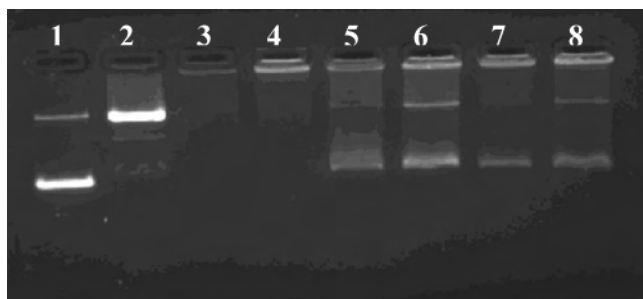


Figure 5. Gel mobility shift assay of *S. cervi* Topo II by complexes **1**, **2**, and **6** (5 μg , lanes 3, 5, and 7; 2 μg , lane 4, 6, and 8). Lane 1: pBR322 (0.25 μg) alone. Lane 2: pBR322 + *S. cervi* Topo II. Lanes 3 and 4: **1**. Lanes 5 and 6: **2**. Lanes 7 and 8: **6**.



Figure 6. Gel mobility shift assay of *S. cervi* Topo II by complexes **2**, **3**, and **7–9** (2 μg , lanes 3, 5, 7, 9, and 11; 0.2 μg , lanes 4, 6, 8, 10, and 12). Lane 1: pBR322 (0.25 μg) alone. Lane 2: pBR322 + *S. cervi* Topo II. Lanes 3 and 4: **2**. Lanes 5 and 6: **3**. Lanes 7 and 8: **7**. Lanes 9 and 10: **8**. Lanes 11 and 12: **9**.

of the chloro group by anionic ligands like SCN^- or N_3^- has little influence on the MLCT bands. The complexes under study are nonluminescent at room temperature.

DNA Interaction Studies. Gel electrophoresis assays were performed to elucidate direct metal–DNA interaction following a shift in the electrophoretic mobility of the plasmid DNA on agarose gel. Metal–DNA interaction causes alteration in the structure of DNA, whereupon the mobility of supercoiled DNA decreases and the migration of open-circular DNA slightly increases at the comigration junction of both forms. Further, an essential cellular enzyme Topo II has been identified as an important biochemical target in chemotherapy and microbial infections, which is intricately involved in the topographic structure of DNA transcription and mitosis.²⁴ Anti-Topo II agents control the Topo II activity either by trapping the Topo II–DNA complex or by acting as Topo II inhibitors.²⁵

The enzyme-mediated supercoiled pBR322 relaxation assay was performed to examine the influence of the complexes on the Topo II–DNA activity of the filarial parasite *S. cervi*.²⁶ Interaction studies exhibited an inhibitory

effect of the metal complexes on the Topo II activity of the filarial parasite. Gel mobility assays of the mono- and dinuclear complexes (**1**, **2**, and **5–9**) were examined at various concentration levels. All of the complexes exhibited DNA binding behavior. An upshift of bound DNA to the gel origin indicated that these complexes greatly influence the Topo II–DNA activity by binding to either the Topo II–DNA complex, DNA, or the enzyme. An appreciable effect on the DNA activity has been observed upon substitution of the chloro group in the parent complex **1**. Complexes **2** and **6** show complex formation as well as inhibitory activity at higher concentration levels of 5 μg , where as parent complex **1** shows inhibitory activity only below 0.2 μg levels (Figure 5). The homo/heterodinuclear complexes show a strong ability toward complex formation with the DNA–Topo II complex even at concentrations lower than 2 μg (Figure 6). The DNA topoisomerase inhibitory activity of the complexes under study was found to be concentration-dependent. At concentrations lower than 0.2 μg (or below at 0.02 and 0.05 μg levels), the complexes induce relaxation of the supercoiled DNA, displaying a significant inhibitory activity of 50–60% as shown in Figure 7. The inhibition percentage was reduced to \sim 40% at 0.02 μg concentration. However, if the concentration was reduced further, no inhibitory activity was observed.

Anomalous morphology of Z–DNA and its involvement in gene expression and recombination has drawn enormous scientific attention on B–Z transitions.²⁷ The B \rightarrow Z form conversion in the presence of the complexes under study was followed spectrophotometrically. All of the complexes (except **6**) promote conformational changes in the structure of DNA from B \rightarrow Z form as evidenced by the observed change in the A_{260}/A_{295} ratio from 2.17 for free DNA to 1.32 (**1**), 1.18 (**2**), 1.18 (**3**), 2.61 (**6**), 1.20 (**7**), 1.50 (**8**), and 1.27 (**9**). Further, condensation of calf thymus (CT) DNA induced by the complexes was monitored spectroscopically following the increase in the absorption value at 320 nm.²⁸ All of the complexes (except **6**) were found to cause condensation of DNA at 10–20 μg concentration. The condensation of DNA was monitored by measuring the increase in the value of absorption at 320 nm [0.029 for free DNA to 0.149 (**1**), 0.123 (**2**), 0.127 (**3**), 0.010(**6**), 0.139 (**7**), 0.129 (**8**), and 0.133 (**9**)] or a decrease in the absorbance at 260 nm. Complexes **1** and **2** at 10 μg concentration caused condensation of DNA, while complex **6** was not effective in this process.

Ruthenium(II) polypyridyl complexes **1–3** and **6–9** also displayed a significant inhibitory effect on the heme polymerase activity of *P. yoelii* lysate, which was studied by β -hematin formation.²⁹ The parent mononuclear complex **1** showed 94% inhibition of the heme polymerase activity, while complexes **2**, **3**, and **6–9** exhibited 71, 38, 23, 45, 34, and 18% inhibition, respectively. The observed result could be attributed to an increase in the steric hindrance by

(24) Wang, J. C. *J. Biol. Chem.* **1991**, *266*, 6659.

(25) Morris, R. E.; Aird, R. E.; Murdoch, P. del S.; Chen, H.; Cummings, J.; Hughes, N. D.; Parsons, S.; Parkin, A.; Boyd, G.; Jodrell, D. I.; Sadler, P. J. *J. Med. Chem.* **2001**, *44*, 3616.

(26) (a) Pandya, U.; Saxena, J. K.; Kaul, S. M.; Murthy, P. K.; Chatterjee, R. K.; Tripathi, R. P.; Bhaduri, A. P.; Shukla, O. P. *Med. Sci. Res.* **1999**, *27*, 103. (b) Tripathi, R. P.; Rastogi, S. K.; Kundu, B.; Saxena, J. K.; Reddy, V. J. M.; Shrivastav, S. K.; Chandra, S.; Bhaduri, A. P. *Comb. Chem. High Throughput Screening* **2001**, *4*, 237. (c) Burden, D. A.; Osheroff, N. *Biochim. Biophys. Acta* **1998**, *1400*, 139.

(27) (a) Pohl, E. M.; Jovin, T. M. *J. Mol. Biol.* **1972**, *67*, 375. (b) Chaires, J. B. *J. Biol. Chem.* **1986**, *261*, 8899 and references cited therein.

(28) (a) Basu, H. S.; Marton, L. J. *Biochem. J.* **1987**, *244*, 243. (b) Thomas, T. J.; Messner, R. P. *J. Mol. Biol.* **1988**, *201*, 463.

(29) Pandey, A. V.; Singh, N.; Takwani, B. L.; Puri, S. K.; Chauhan, V. S. *J. Pharm. Biomed. Anal.* **1999**, *20*, 203.

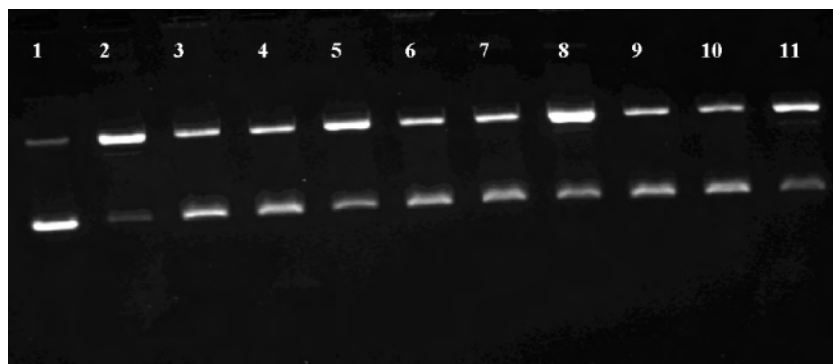


Figure 7. Gel mobility shift assay of *S. cervi* Topo II by complexes **1**, **2**, and **6** (0.2 μg , lanes 3, 6, and 9; 0.05 μg , lanes 4, 7, and 10; 0.02 μg , lanes 5, 8, and 11). Lane 1: pBR322 (0.25 μg) alone. Lane 2: pBR322 + *S. cervi* Topo II. Lanes 3–5: **1**. Lanes 6–8: **2**. Lanes 9–11: **6**.

subsequent replacement of the chloro group in **1** and incorporation of another metal center in **7–9** reducing the free coordination sites.

Conclusion

In this work, we have presented the synthesis and spectral and structural characterization of some neutral and cationic ruthenium(II) polypyridyl complexes with multifaceted values. The complex $[\text{Ru}(\kappa^3\text{-tptz})(\text{PPh}_3)\text{Cl}_2]$ exhibits a rich chemistry, serves as a good precursor to form interesting substitutional products, and acts as a potential *metalloligand* in the synthesis of homo- and heterodinuclear complexes. Further, the complexes exhibit inhibitory activity against the Topo II–DNA interaction of filarial parasite *S. cervi* and β -hematin/hemozoin formation in the presence of *P. yoelii* lysate.

Experimental Section

Reagents. All of the synthetic manipulations were performed under a nitrogen atmosphere in deaerated solvents. The solvents were purified rigorously by standard procedures prior to their use.³⁰ Ammonium tetrafluoroborate, triphenylphosphine, bis(diphenylphosphino)methane, sodium diethyldithiocarbamate, sodium azide, potassium thiocyanate, 1,3-cyclohexadiene, α -phellandrene, pentamethylpentacyclodiene, ruthenium(III) chloride hydrate, and rhodium(III) chloride hydrate (all from Aldrich) were used as received without further purification. Arene ruthenium complexes $[\{\eta^6\text{-C}_6\text{H}_6\}\text{Ru}(\mu\text{-Cl})\text{Cl}]_2$ and $[\{\eta^6\text{-C}_{10}\text{H}_{14}\}\text{Ru}(\mu\text{-Cl})\text{Cl}]_2$ and isostructural rhodium complex $[\{\eta^5\text{-C}_5\text{Me}_5\}\text{Rh}(\mu\text{-Cl})\text{Cl}]_2$ were prepared and purified by literature procedures.³¹ Triply distilled deionized water was used for the preparation of various buffers. Calf thymus (CT) DNA and supercoiled pBR322 DNA was procured from Sigma Chemical Co., St. Louis, MO. Topoisomerase II (Topo II) from the filarial parasite *S. cervi* was partially purified according to the method by Pandya et al.²⁶

General Methods. Elemental analyses were performed by the Microanalytical Section of the Sophisticated Analytical Instrumentation Centre, Central Drug Research Institute, Lucknow, India. IR in KBr disks and electronic spectra for a dichloromethane solution

of the complexes were recorded on Shimadzu 8201PC and UV-1601 spectrophotometers, respectively. ^1H and ^{31}P NMR spectra were recorded on a Bruker DRX-300 NMR instrument. Tetramethylsilane and phosphorus trichloride have been used as internal references for ^1H and ^{31}P NMR spectroscopic studies, respectively. FAB-MS spectra were recorded on a JEOL SX 102/DA 6000 mass spectrometer using xenon (6 kV, 10 mA) as the FAB gas. The accelerating voltage was 10 kV, and the spectra were recorded at room temperature with *m*-nitrobenzyl alcohol as the matrix.

Synthesis of $[\text{Ru}(\kappa^3\text{-tptz})(\text{PPh}_3)\text{Cl}_2]$ (1**).** A suspension of $[\text{RuCl}_2(\text{PPh}_3)_3]$ (0.990 g, 1.0 mmol) in benzene (35 mL) was treated with tptz (0.312 g, 1.0 mmol), and the resulting solution was heated under reflux for 4 h, whereupon a microcrystalline product separated from the blue solution. The microcrystalline product was collected by filtration, washed repeatedly with benzene and diethyl ether, and dried under vacuum. Yield: 0.671 g (90%). Anal. Calcd for $\text{C}_{36}\text{Cl}_2\text{H}_{27}\text{N}_6\text{PRu}$: C, 57.90; H, 3.61; N, 11.26. Found: C, 58.12; H, 3.40; N, 11.41. FAB-MS (obsd (calcd), rel intens, assignments): m/z 710 (711), 50, $[\text{Ru}(\kappa^3\text{-tptz})(\text{PPh}_3)\text{Cl}]^+$; 674 (675), 25, $[\text{Ru}(\kappa^3\text{-tptz})(\text{PPh}_3)]^{2+}$; 412 (413), 12, $[\text{Ru}(\kappa^3\text{-tptz})]^{2+}$. ^1H NMR (300 MHz, CDCl_3): δ 9.46 (d, 2H, $J = 4.2$ Hz), 8.95 (d, 1H, $J = 2.7$ Hz), 8.61 (dd, 3H, $J = 8.7$ Hz), 7.96 (t, 1H, $J = 6.9$ Hz), 7.86 (t, 2H, $J = 6.9$ Hz), 7.55 (m, 3H), 7.36–7.10 (br m, 15H, PPh_3). ^{31}P - $\{^1\text{H}\}$ NMR: δ 36.69 (s). UV–vis [CH_2Cl_2 ; λ_{max} , nm (ϵ , $\text{M}^{-1}\text{cm}^{-1}$): 534 (7260), 371 (6360), 288 (26 270).

Synthesis of $[\text{Ru}(\kappa^3\text{-tptz})(\kappa^2\text{-dppm})\text{Cl}]\text{BF}_4$ (2**).** A suspension of **1** (0.746 g, 1.0 mmol) in methanol (25 mL) was treated with dppm (0.384 g, 1.0 mmol) and refluxed for 4 h. The resulting bright-orange-red solution was filtered to remove any solid impurities, treated with a saturated solution of NH_4BF_4 in methanol, and left for slow crystallization. The orange-red crystalline product was separated by filtration and washed with methanol and diethyl ether. Yield: 0.672 g (73%). Anal. Calcd for $\text{BC}_{45}\text{ClF}_4\text{H}_{34}\text{N}_6\text{P}_2\text{Ru}$: C, 56.08; H, 3.69; N, 9.13. Found: C, 56.39; H, 4.03; N, 9.51. FAB-MS (obsd (calcd), rel intens, assignments): m/z 833 (833), 75, $[\text{Ru}(\kappa^3\text{-tptz})(\kappa^2\text{-dppm})\text{Cl}]^+$; 797 (797), 80, $[\text{Ru}(\kappa^3\text{-tptz})(\kappa^2\text{-dppm})]^{2+}$; 413 (413), 25, $[\text{Ru}(\kappa^3\text{-tptz})]^{2+}$. ^1H NMR (300 MHz, CDCl_3): δ 9.00 (t, 4H, $J = 7.2$ Hz), 8.37 (m, 3H), 8.12 (d, 1H, $J = 6.0$ Hz), 7.89 (t, 2H, $J = 7.5$ Hz), 7.59 (td, 2H, $J = 4.8$ Hz), 7.27–6.82 ppm (br m, 20H, dppm), 5.50 (m, 2H of dppm). $^{31}\text{P}\{^1\text{H}\}$ NMR: δ 6.64 (d, $J = 56.62$ Hz), -11.29 (d, $J = 58.56$ Hz). IR (cm^{-1} , Nujol): $\nu(\text{BF}_4^-)$ 1060. UV–vis [CH_2Cl_2 ; λ_{max} , nm (ϵ , $\text{M}^{-1}\text{cm}^{-1}$): 478 (6970), 295 (27 180).

Alternatively, complex **2** was also prepared by the reaction of $[\text{Ru}(\kappa^3\text{-tptz})(\text{PPh}_3)_2\text{Cl}]\text{BF}_4$ with dppm in methanol under refluxing conditions.^{14a}

(30) Perrin, D. D.; Armango, W. L. F.; Perrin, D. R. *Purification of laboratory Chemicals*; Pergamon: Oxford, U.K., 1986.

(31) (a) Robertson, D. R.; Robertson, I. W.; Stephenson, T. A. *J. Organomet. Chem.* **1980**, 202, 309. (b) Bennett, M. A.; Smith, A. K. *J. Chem. Soc., Dalton Trans.* **1974**, 233. (c) Bennett, M. A.; Huang, T.-N.; Matheson, T. W.; Smith, A. K. *Inorg. Synth.* **1982**, 21, 74. (d) White, C.; Yates, A.; Maitilis, P. M. *Inorg. Synth.* **1992**, 29, 228.

Synthesis of [Ru(κ^3 -tptz)(PPh₃)(pa)]Cl (3). A suspension of **1** (0.746 g, 1.0 mmol) in methanol (25 mL) was treated with a methanol solution of phenylalanine (pa; 0.165 g, 1.0 mmol) and KOH (0.056 g, 1.0 mmol) and refluxed for 4 h. The resulting violet-black solution was filtered while hot to remove any solid impurities and left for slow crystallization. After a few days, a microcrystalline product appeared. It was separated by filtration and washed with diethyl ether. Yield: 0.656 g (75%). Anal. Calcd for C₄₅H₃₇N₇O₂-PRu: C, 61.71; H, 4.23; N, 11.20. Found: C, 61.49; H, 4.41; N, 11.31. ¹H NMR (300 MHz, CDCl₃): δ 8.93 (d, 1H, J = 4.5 Hz), 8.62 (m, 5H), 7.95 (m, 2H), 7.79 (t, 1H, J = 7.7 Hz), 7.53 (m, 2H), 7.28 (t, 3H, J = 5.1 Hz), 7.12 (br m for 2H of the Ph ring of pa and 15H of PPh₃), 3.53 (m, 1H), 2.77 (d, 2H, J = 4.8 Hz). ³¹P{¹H} NMR: δ 40.77 (s). IR (cm⁻¹, Nujol): ν (CO) 1627, 1720. UV-vis [CH₂Cl₂; λ_{max} , nm (ϵ , M⁻¹ cm⁻¹): 491 (8840), 355 (7560), 276 (23 340).

Synthesis of [Ru(κ^3 -tptz)(PPh₃)(dte)]Cl (4). A suspension of **1** (0.746 g, 1.0 mmol) and sodium diethyldithiocarbamate (0.224 g, 1.0 mmol) in methanol was refluxed for 6 h. The resulting solution was completely evaporated to dryness on a water bath. The solid mass thus obtained was extracted with dichloromethane and precipitated with diethyl ether. Yield: 0.653 g (76%). Anal. Calcd for C₄₁H₃₇N₇PRuS₂: C, 57.24; H, 4.30; N, 11.40. Found: C, 56.98; H, 4.39; N, 11.09. FAB-MS (obsd (calcd); rel intens; assignment): m/z 824 (823), 75, [Ru(κ^3 -tptz)(PPh₃)(dte)]⁺; 561 (562), 60, [Ru(κ^3 -tptz)(dte)]⁺; 414 (413), 25, [Ru(κ^3 -tptz)]²⁺. ¹H NMR (300 MHz, CDCl₃): δ 9.12 (dd, 4H, J = 5.4 Hz), 8.93 (d, 2H, J = 5.1 Hz), 8.19 (t, 2H, J = 5.7 Hz), 7.76 (t, 2H, J = 6.0 Hz), 6.99 (t, 2H, J = 9.3 Hz), 7.36–7.10 (br m, 15H, PPh₃), 4.11 (q, 2H, J = 6.9 Hz), 3.59 (q, 2H, J = 7.2 Hz), 1.52 (t, 3H, J = 7.2 Hz), 1.12 (t, 3H, J = 6.9 Hz). ³¹P{¹H} NMR: δ 38.48 (s). IR (cm⁻¹, Nujol): ν (CS) 1207. UV-vis [CH₂Cl₂; λ_{max} , nm (ϵ , M⁻¹ cm⁻¹): 485 (9580), 353 (9480), 290 (24 980).

Synthesis of [Ru(κ^3 -tptz)(PPh₃)(SCN)₂] (5). It was synthesized from the reaction of **1** (0.746 g, 1.0 mmol) with a slight excess of NH₄SCN in methanol under refluxing conditions. The reaction mixture was cooled to room temperature and filtered. The solid was washed with methanol and diethyl ether. Yield: 0.554 g (70%). Anal. Calcd for C₃₈H₂₇N₈PRuS₂: C, 57.64; H, 3.69; N, 9.13. Found: C, 57.47; H, 4.01; N, 9.50. FAB-MS (obsd (calcd), rel intens, assignments): m/z 792 (791), 50, [Ru(κ^3 -tptz)(PPh₃)(SCN)₂]; 734 (733), 95, [Ru(κ^3 -tptz)(PPh₃)(SCN)]⁺; 675 (675), 25, [Ru(κ^3 -tptz)(PPh₃)]²⁺; 413 (413), 20, [Ru(κ^3 -tptz)]²⁺. ¹H NMR (300 MHz, CDCl₃): δ 9.01 (dd, 2H, J = 5.7 Hz), 8.62 (dd, 2H, J = 4.8 Hz), 8.02 (t, 1H, J = 7.2 Hz), 7.97 (d, 1H, J = 6.6 Hz), 7.92 (d, 2H, J = 6.9 Hz), 7.61 (t, 3H, J = 6.0 Hz), 9.31 (d, 1H, J = 5.1 Hz), 7.34–7.13 (br m, 15H, PPh₃). ³¹P{¹H} NMR: δ 36.84 (s). IR (cm⁻¹, Nujol): ν (SCN) 2092. UV-vis [CH₂Cl₂; λ_{max} , nm (ϵ , M⁻¹ cm⁻¹): 516 (7880), 355 (8260), 274 (30 100).

Synthesis of [Ru(κ^3 -tptz)(PPh₃)(N₃)₂] (6). Complex **6** was prepared by the reaction of **1** with a slight excess of sodium azide in methanol according to the procedure adopted for **5**. Yield: 0.577 g (76%). Anal. Calcd for C₃₆H₂₇N₁₂PRu: C, 56.91; H, 3.55; N, 22.13. Found: C, 57.11; H, 3.71; N, 21.95. ¹H NMR (300 MHz, CDCl₃): δ 9.47 (d, 2H, J = 5.4 Hz), 8.96 (d, 1H, J = 4.2 Hz), 8.59 (dd, 3H, J = 7.8 Hz), 7.86 (t, 3H, J = 6.6 Hz), 7.59 (m, 3H), 7.34–7.10 (br m, 15H, PPh₃). ³¹P{¹H} NMR: δ 36.20 (s). IR (cm⁻¹, Nujol): ν (N₃) 2011–2037. UV-vis [CH₂Cl₂; λ_{max} , nm (ϵ , M⁻¹ cm⁻¹): 558 (5450), 374 (5770), 282 (23 700).

Synthesis of [Cl₂(PPh₃)Ru(μ -tptz)Ru(η^6 -C₆H₆)Cl]BF₄ (7). To a suspension of **1** (0.746 g, 1.0 mmol) in methanol (25 mL) was added [(η^6 -C₆H₆)Ru(μ -Cl)Cl]₂ (0.250 g, 0.5 mmol), and the resulting suspension was refluxed for 4 h. Slowly the complex [-(

(η^6 -C₆H₆)Ru(μ -Cl)Cl]₂] dissolved and gave a blue-black solution. The reaction mixture was cooled to room temperature, and a saturated solution of NH₄BF₄ in methanol was added and left for slow crystallization. A blue-black crystalline product was separated by filtration, washed with diethyl ether, and dried under vacuum. Yield: 0.734 g (70%). Anal. Calcd for BC₄₂Cl₃FH₃₃N₆PRu₂: C, 48.09; H, 3.14; N, 8.01. Found: C, 47.86; H, 3.51; N, 7.77. FAB-MS (obsd (calcd), rel intens, assignments): m/z 961 (961), 45, [Cl₂(PPh₃)Ru(μ -tptz)Ru(η^6 -C₆H₆)Cl]⁺; 698 (699), 40, [Cl₂Ru(μ -tptz)-Ru(η^6 -C₆H₆)Cl]⁺. ¹H NMR (300 MHz, CDCl₃): δ 10.53 (d, 1H, J = 7.8 Hz), 9.54 (d, 1H, J = 5.1 Hz), 9.39 (d, 1H, J = 5.1 Hz), 9.19 (d, 1H, J = 5.4 Hz), 8.62 (m, 2H), 8.25 (t, 1H, J = 7.8 Hz), 8.08 (m, 3H), 7.83 (t, 1H, J = 4.2 Hz), 7.57 (t, 1H, J = 7.2 Hz), 7.26–7.14 (br m, 15H, PPh₃), 5.82 (s, 6H, C₆H₆). ³¹P{¹H} NMR: δ 29.91 (s). IR (cm⁻¹, Nujol): ν (BF₄⁻) 1060. UV-vis [CH₂Cl₂; λ_{max} , nm (ϵ , M⁻¹ cm⁻¹): 590 (10 130), 404 (7120), 300 (23 230).

Synthesis of [Cl₂(PPh₃)Ru(μ -tptz)Ru(η^6 -C₁₀H₁₄)Cl]PF₆ (8). Complex **8** was prepared by the reaction of **1** with [(η^6 -C₁₀H₁₄)Ru(μ -Cl)Cl]₂ (0.306 g, 0.5 mmol) in methanol according to the procedure for **7**. Yield: 0.872 g (75%). Anal. Calcd for C₄₆-Cl₃F₆H₄₁N₆PRu₂: C, 47.50; H, 3.52; N, 7.22. Found: C, 47.15; H, 3.88; N, 6.97. FAB-MS (obsd (calcd), rel intens, assignments): m/z 1018 (1017), 99, [Cl₂(PPh₃)Ru(μ -tptz)Ru(η^6 -C₁₀H₁₄)Cl]⁺; 755 (755), 60, [Cl₂Ru(μ -tptz)Ru(η^6 -C₁₀H₁₄)Cl]⁺. ¹H NMR (300 MHz, CDCl₃): δ 10.64 (d, 1H, J = 7.8 Hz), 9.68 (d, 1H, J = 4.8 Hz), 9.48 (d, 1H, J = 5.4 Hz), 9.41 (d, 1H, J = 7.5 Hz), 8.63 (m, 2H), 8.26 (t, 1H, J = 7.8 Hz), 8.05 (m, 3H), 7.82 (t, 1H, J = 4.2 Hz), 7.56 (t, 1H, J = 7.2 Hz), 7.26–7.14 (br m, 15H, PPh₃), 5.69 (m, 3H), 5.45 (d, 1H, J = 5.4 Hz), 2.65 (m, 1H, CH₃CH₂CH₃), 2.12 (s, 3H, CCH₃), 1.09 (d, 3H, J = 6.3 Hz, CH(CH₃)₂), 0.92 (d, 3H, J = 6.6 Hz, CH(CH₃)₂). ³¹P{¹H} NMR: δ 27.89 (s). IR (cm⁻¹, Nujol): ν (PF₆⁻) 842. UV-vis [CH₂Cl₂; λ_{max} , nm (ϵ , M⁻¹ cm⁻¹): 595 (10 790), 410 (7300), 300 (22 650).

Synthesis of [Cl₂(PPh₃)Ru(μ -tptz)Rh(η^5 -C₅Me₅)Cl]BF₄ (9). Complex **9** was prepared by the reaction of **1** with [(η^5 -C₅Me₅)Rh(μ -Cl)Cl]₂ (0.309 g, 0.5 mmol) in methanol according to the procedure for **7**. Yield: 0.809 g (73%). Anal. Calcd for BC₄₆-Cl₃F₆H₄₂N₆RuRh: C, 49.86; H, 3.79; N, 7.58. Found: C, 50.01; H, 4.10; N, 7.46. FAB-MS (obsd (calcd), rel intens, assignments): m/z 1021 (1020), 80, [Cl₂(PPh₃)Ru(μ -tptz)Rh(η^5 -C₅Me₅)Cl]⁺; 985 (986), 30, [Cl₂(PPh₃)Ru(μ -tptz)Rh(η^5 -C₅Me₅)]²⁺. ¹H NMR (300 MHz, CDCl₃): δ 10.54 (d, 1H, J = 7.8 Hz), 9.62 (d, 1H, J = 5.1 Hz), 9.46 (d, 1H, J = 5.1 Hz), 9.20 (d, 1H, J = 5.4 Hz), 9.05 (d, 1H, J = 7.8 Hz), 8.85 (d, 1H, J = 7.5 Hz), 8.60 (t, 1H, J = 7.5 Hz), 8.30 (m, 3H), 8.10 (t, 1H, J = 5.7 Hz), 7.94 (t, 1H, J = 5.7 Hz), 7.40–7.34 (br m, 15H, PPh₃), 1.45 (s, 15H, C₅(CH₃)₅). ³¹P{¹H} NMR: δ 29.81 (s). IR (cm⁻¹, Nujol): ν (BF₄⁻) 1060. UV-vis [CH₂Cl₂; λ_{max} , nm (ϵ , M⁻¹ cm⁻¹): 589 (6290), 408 (4550), 293 (19 710).

Crystal Structure Determinations. Crystals suitable for single-crystal X-ray analyses for complexes **1–3**, **8**, and **9** were grown from CH₂Cl₂/petroleum ether (40–60 °C) at room temperature. Preliminary data on the space group and unit cell dimensions as well as intensity data were collected on an Enraf-Nonius MACH3 diffractometer using graphite-monochromatized Mo K α radiation. The crystal orientation, cell refinement, and intensity measurements were made using the program CAD-4 PC. The structures were solved by direct methods and refined by using SHELX-97.³² The non-hydrogen atoms were refined with anisotropic thermal parameters. All of the hydrogen atoms were geometrically fixed and

(32) Sheldrick, G. M. SHELX-97: Programme for the solution and refinement of crystal structures; University of Göttingen: Göttingen, Germany, 1997.

allowed to refine using a riding model. The computer program *PLATON* was used for analyzing the interaction and stacking distances.³³

Gel Mobility Shift Assays. The enzymatic activity of Topo II was monitored by relaxation of supercoiled pBR322 DNA.^{26a,c} For relaxation assay, the reaction mixture (20 μ L) contained 50 mM Tris-HCl, pH 7.5, 50 mM KCl, 1 mM MgCl₂, 1 mM ATP, 0.1 mM EDTA, 0.5 mM DTT, 30 μ g/mL BSA, and enzyme protein. Supercoiled pBR322 DNA (0.25 μ g) was used as the substrate. The reaction mixture was incubated for 30 min at 37 °C and stopped by the addition of 5 μ L of loading buffer containing 0.25% bromophenol blue, 1 M sucrose, 1 mM EDTA, and 0.5% SDS. Samples were applied on horizontal 1% agarose gel in 40 mM Tris-acetate buffer, pH 8.3, and 1 mM EDTA and run for 10 h at room temperature at 20 V. The gel was stained with ethidium bromide (0.5 μ g/mL) and photographed in a GDS 7500 UVP (Ultra Violet Products, Cambridge, U.K.) transilluminator. One unit of topoisomerase activity is defined as the amount of enzyme required to relax 50% of the supercoiled DNA under the standard assay conditions.

The conformational transition of CT DNA in the presence of the complexes was determined spectrophotometrically.^{27a} The UV absorbance ratio of A_{260}/A_{295} was monitored for conformational change in the DNA helix from B \rightarrow Z DNA. Condensation of DNA was monitored by following the increase in the value of absorbance at 320 nm (A_{320}) against different complex/DNA ratios, according to the method of Basu and Marton.^{28a}

Heme Polymerase Assay. Anti-malarial activity of the complexes was studied by the respective inhibition percentage against β -hematin formation.²⁹ The reaction mixture in 1 mL contained 100 μ L of 1 M sodium phosphate buffer, 20 μ L of hemin (1.2 mg/

mL), and 25 μ L of *P. yoelii* enzyme, and the volume was made up with triple-distilled water. A total of 20 μ g of the complexes was added in the reaction mixture and incubated for 16 h at 37 °C in an incubator shaker at a speed of 174 rpm. After incubation, the reaction mixture was centrifuged at 10 000 rpm for 15 min and the pellets obtained were washed three times with 10 mL of buffer containing 0.1 M Tris-Cl buffer, pH 7.5, and 2.5% SDS and then with buffer 2 (0.1 M sodium bicarbonate buffer, pH 9.2, and 2.5% SDS), followed by distilled water. The semidried pellets were suspended in 50 μ L of 2 N NaOH, and the volume was adjusted to 1 mL with distilled water. The optical density was measured at 400 nm, and the percent inhibition was calculated using the following formula: % inhibition = $\{(1 - \text{o.d. of control})/\text{o.d. of experimental}\} \times 100$.

Acknowledgment. Thanks are due to the Department of Science and Technology, Ministry of Science and Technology, New Delhi, India (Grant SR/S1/IC-15/2006), for providing financial assistance and Prof. P. Mathur, In-charge, National Single-Crystal X-ray Diffraction Facility, Indian Institute of Technology, Mumbai, India, for providing single-crystal X-ray data. We also thank Prof. Q. Xu, UBIQUITOUS Division, AIST, Osaka, Japan, and Dr. J. K. Saxena for their kind help.

Supporting Information Available: Crystallographic data of complexes **1–3**, **8**, and **9** in CIF format and relevant matrixes and figures for weak interactions (Table S1 and Figures S1 and S2, respectively). This material is available free of charge via the Internet at <http://pubs.acs.org>.

IC701518E

(33) Spek, A. L. *Acta Crystallogr.* **1990**, *46*, C31.